ELSEVIER

Journal of Marine Systems 20 (1999) 157–173

JOURNAL OF MARINE SYSTEMS

Modelling the Mediterranean Sea: climatological forcing

P.G. Drakopoulos *, A. Lascaratos

Laboratory of Meteorology and Oceanography, Department of Applied Physics, University of Athens, Athens, Greece

Received 31 March 1997; accepted 26 August 1997

Abstract

Within the framework of a Mediterranean model evaluation experiment, a Princeton Ocean Model (POM) of the Mediterranean has been developed in University of Athens. In this paper, the results of the coarse resolution version ($1/4° \times 1/4°$) are presented. SST and SSS were restored to monthly climatology with a time constant of 1 m day^{-1}. The seasonal variability of the general circulation was found to be in a good agreement with the observed patterns and some known features have been modelled for the first time. The implied surface fluxes (heat loss and salt gain) were too weak and resulted in absence of deep water formation.

Keywords: Mediterranean Sea; Princeton Ocean Model (POM); regional basin

1. Introduction

In strictly geographical terms, the Mediterranean Sea is considered a regional basin. However, the presence of almost all the important physical oceanographic processes with the additional simplicity of the well controlled fluxes due to its semi-enclosed nature, renders the basin a scale model for oceanographers. Thus, considerable effort has been put up to this day, in order to understand, explain and emulate the observed structures and their driving mechanisms.

In Fig. 1, the geography of the Mediterranean Sea and the nomenclature of the major subbasins and straits are depicted. The Mediterranean is connected to the Atlantic through the narrow Strait of Gibraltar which has a width of about 13 km and depth at the sill of about 300 m. It is composed of two subbasins, the Western and Eastern which communicate via the Strait of Sicily, with width of 140 km and average depth of 500 m. Due to the excess evaporation over precipitation and runoff (0.6 myr^{-1}, Bryden and Kinder, 1991), the basin behaves as a concentration basin (lagoon). The water deficit is made up by an excess inflow of relatively fresh and warm Atlantic water (NAW) through Gibraltar. The Atlantic water transports heat through the strait and balances the loss through the entire surface of the basin (7 ± 3 W m^{-2}, e.g., Bethoux, 1979). The inflow generates the Atlantic stream system which in its way to the eastern-most part of the basin evolves into the Algerian current, the Ionian–Atlantic stream and finally the Mid Mediterranean Jet. This system divides the basin in two parts—the northern and predominately cyclonic and the southern and anticyclonic. In the northern part of each subbasin, there exist two major cyclonic gyres. In the western basin is the Lyon Gyre at the region of the Gulf of Lions where west

* Corresponding author. Institute of Marine Biology of Crete, P.O. Box 2214, 71003 Iraklio, Crete, Greece. Tel.: +30-81-34860; Fax: +30-81-241882; E-mail: pdrak@imbc.gr

0924-7963/99/$ - see front matter
PII: S0924-7963(98)00080-3

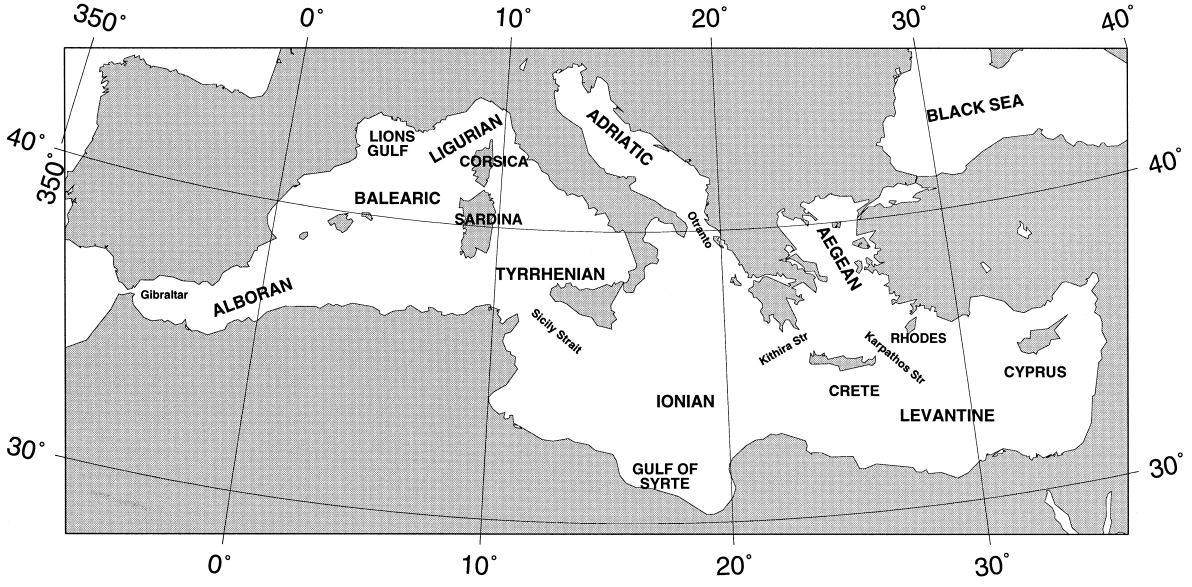

Fig. 1. The geography of the Mediterranean Sea.

Mediterranean deep waters are formed. In the eastern basin is the Rhodes Gyre, south of the island of Rhodes in the Levantine, where intermediate waters are formed and travel westward to eventually outflow through Gibraltar. Other cyclonic gyres that exist are the Tyrrhenian Gyre, the western Ionian Gyre, the south Adriatic Gyre where some of the deep East Mediterranean waters are formed, and the western Cretan Gyre southwest of the island of Crete. Finally, a series of major anticyclonic gyres exist, the Alboran Gyre, the Mersa–Matruh Gyre in the southern Levantine, the Shikmona Gyre in the south–east Levantine, and the Pelops Gyre, off the south–west tip of Peloponesus. The general circulation of the basin and its large scale properties have been reviewed recently by Robinson and Golnaraghi (1994) where a more detailed description can be found.

It is evident from the complicated patterns of the circulation that the Mediterranean poses as a challenge for numerical modelling. It is not strange therefore that a fair number of efforts have been attempted so far towards modelling the particular basin. A first attempt focused on the barotropic wind driven circulation and was carried out by Menzin and Moskalenko (1982). Later, Stanev et al. (1989) presented a model with very coarse resolution and the Strait of Gibraltar closed and investigated the seasonal variability of the circulation. More recently, Pinardi and Navarra (1993) developed a Mediterranean model based on the *MOM* (Modular Ocean Model) code, an evolution of the Bryan Cox model. In its initial configuration the Gibraltar strait was closed, sea surface temperature (*SST*) and sea surface salinity (*SSS*) were kept frozen to the annual mean value and it was forced only with monthly surface wind stress. In that paper, the baroclinic wind adjustment processes were investigated and the multiple time-scale character of the basin was established. Later, an improved version of this model was presented by Roussenov et al. (1995), (hereinafter referred to as RSAP). This was also a coarse resolution version ($1/4° \times 1/4°$) of the *MOM* code, but now surface forcing included interactively forced heat flux from bulk formulae and salinity relaxation to climatology. An eddy producing version of this model (achieved through reduction of horizontal diffusivity) but with *SST* and *SSS* restoration to climatology, have been reported by Wu and Haines (1996). Meanwhile, Zavatarelli and Mellor (1995) (hereinafter referred to as ZM), presented a *POM* (Princeton Ocean Model) Mediterranean model version with a curvilinear grid. In addition to wind stress forcing, prescribed heat and salt fluxes were imposed on the

surface. All these efforts, have only partially succeeded in realistically and simultaneously simulating the general and the thermohaline circulation, while keeping the heat and water budget of the basin within the observed values. It is an indication of the complexity of the processes present in the basin. Other works have focused on separate subbasins of the Mediterranean. Thus, Malanotte-Rizzoli and Bergamasco (1989, 1991) presented a four layer model for the eastern basin. A model specific for western Mediterranean (Euromodel) was developed by Crepon and Martel (1996). Other work was carried out in order to assess the effect of the interannual variability of the external forcing on the Mediterranean circulation. Thus, a higher resolution in the vertical version of the model by RSAP has been developed, forced with daily NMC winds spanning the period 1981–1987 (Pinardi et al., 1997).

In this work, we present a new modelling effort, by the University of Athens, within the framework of a Mediterranean model intercomparison project (*MEDMEX*, Beckers et al., 1996). The novelty of this study is related to the improved forcing fields that were applied, and which resulted in the reproduction for the first time of some features known to exist in the seasonal variability of the general circulation of the basin. The results we examine here come from a perpetually forced for 15 years model based on the *POM* code. It has a $1/4^\circ \times 1/4^\circ$ resolution in latitude and longitude, with surface relaxation of temperature and salinity. We examine the implied surface heat and water fluxes, the general circulation, the thermohaline circulation, and the transport of properties through the important straits of the basin.

2. Modelling details

The model utilized in this work is the Princeton Ocean Model (*POM*), i.e., Blumberg and Mellor (1987). It is a primitive equation model, with the addition of a free surface (barotropic mode). Technically, this is handled by means of a split-mode time step, one for the barotropic mode and one for the baroclinic one. The equations solved are:

$$\nabla \cdot \vec{u} = 0 \tag{1a}$$

$$\frac{\partial \vec{u}_h}{\partial t} + (\vec{u} \cdot \nabla)\vec{u}_h + f\hat{k} \times \vec{u}_h = -\frac{1}{\rho_0}\nabla p + \frac{\partial}{\partial z}\left(K_M \frac{\partial \vec{u}_h}{\partial z}\right) + (F_U, F_V) \tag{1b}$$

$$\frac{\partial \theta}{\partial t} + \nabla(\theta \vec{u}) = \frac{\partial}{\partial z}\left(K_H \frac{\partial \theta}{\partial z}\right) + F_\theta \tag{1c}$$

$$\frac{\partial S}{\partial t} + \nabla(S\vec{u}) = \frac{\partial}{\partial z}\left(K_H \frac{\partial S}{\partial z}\right) + F_S \tag{1d}$$

The vertical mixing coefficients K_H for momentum and K_M for tracers are calculated from the scheme developed by Mellor and Yamada (1982).

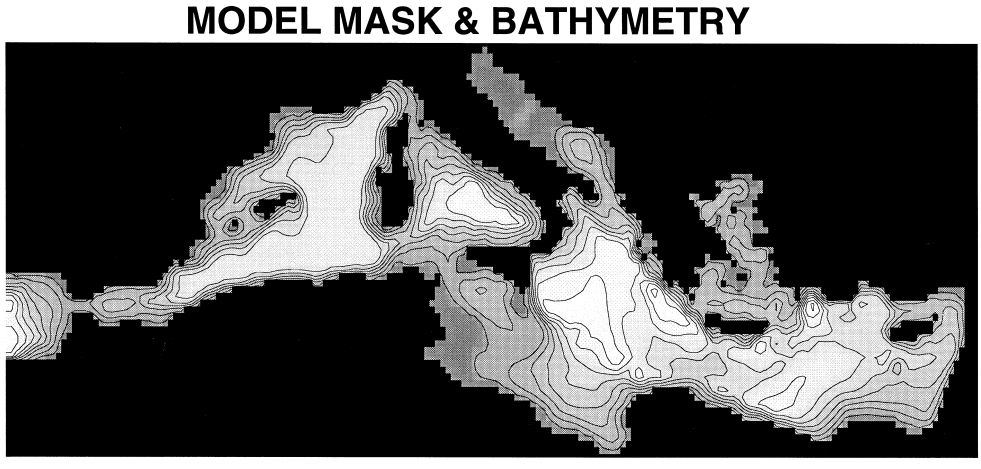

Fig. 2. Bathymetry and mask of the model. Depth in meters.

The horizontal diffusivity terms (F_U, F_V) are evaluated according to the non-linear Smagorinsky algorithm (Smagorinsky, 1963) and are velocity dependent. The surface buoyancy forcing terms F_θ and F_S are given by:

$$F_\theta = \gamma(T* - T) \quad (2a)$$

$$F_S = \gamma(S* - S) \quad (2b)$$

where $T*$ and $S*$ are the climatological restoration values of temperature and salinity, and γ is the restoration time scale. The implied heat and salt fluxes then can be written as:

$$Q_T = \rho c_p \Delta z F_\theta \quad (3a)$$

$$Q_S = \Delta z F_S / S \quad (3b)$$

where Δz is the thickness of the top layer.

The horizontal grid was set with a resolution of $1/4^\circ \times 1/4^\circ$ in longitude and latitude given by $-9.5 + 1/4 \times i$, $i = 1, 182$, and $30 + 1/4 \times j$, $j =$

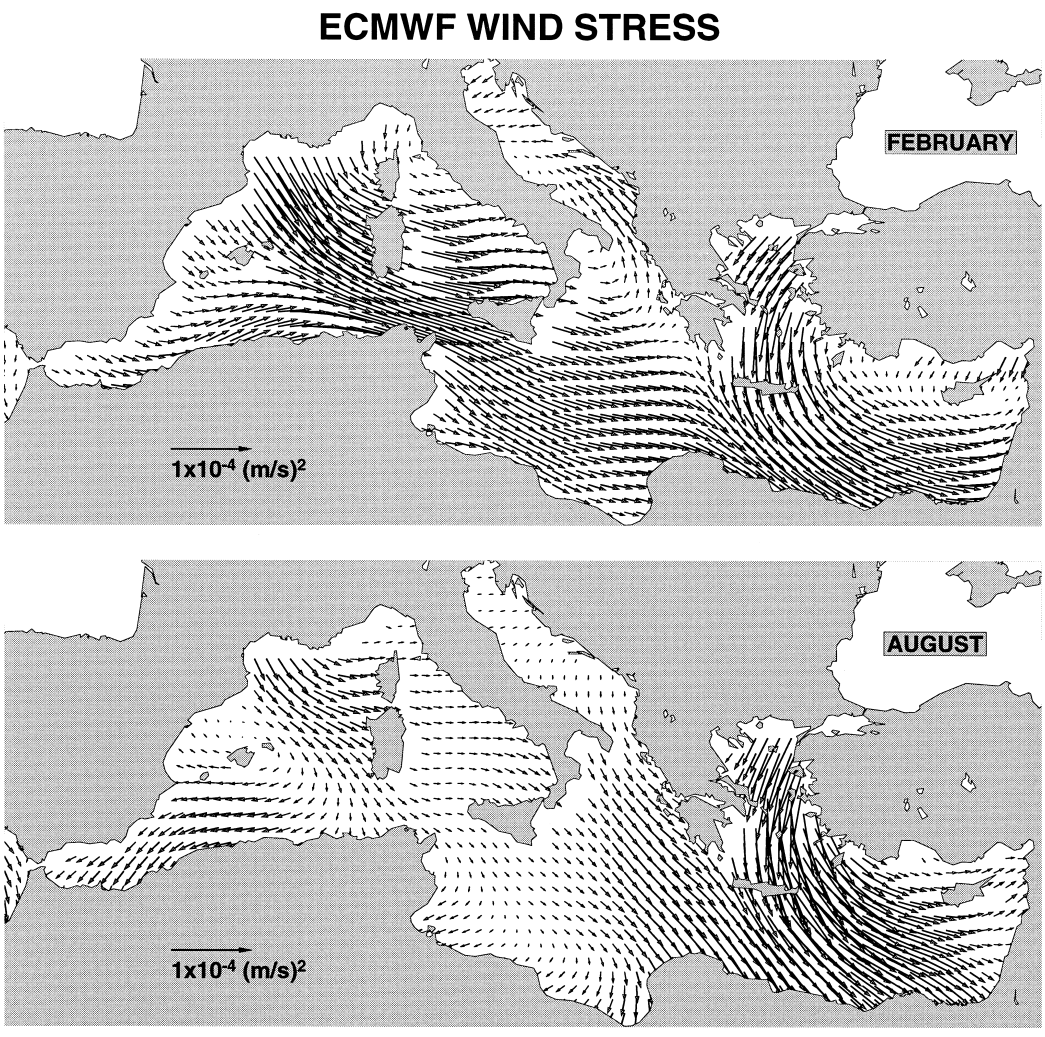

Fig. 3. Wind stress during (a) February and (b) August.

1, 63. In the vertical, 32 sigma levels were chosen having variable resolution being finer near the surface and the bottom. The levels were distributed as: 0, −0.002, −0.005, −0.009, −0.016, −0.026, −0.036, −0.051, −0.071, −0.098, −0.131, −0.166, −0.205, −0.245, −0.285, −0.329, −0.373, −0.417, −0.461, −0.505, −0.549, −0.593, −0.637, −0.681, −0.725, −0.769, −0.813, −0.857, −0.901, −0.945, −0.980, −1. For example, at a nominal depth of 3000 m, the levels were at depths: 0, 6, 15, 27, 48, 78, 108, 153, 213, 294, 393, 498, 615, 735, 855, 987, 1119, 1251, 1383, 1515, 1647, 1779, 1911, 2043, 2175, 2307, 2439, 2571, 2703, 2835, 2940, 3000 (m). The model's bathymetry was interpolated from a blend of the $1/12^{\circ}$ topographies supplied by Harvard and Princeton Universities, both originating from the U.S. Navy. For depths below 500 m, the former was used since is considered best for deep basins and for depths above 200 m the latter which in turn is considered more accurate for shallow basins. In between, a linear weighting of the two data sets was used (i.e., Beckers et al., 1996). Finally, the bathymetry was smoothed with a 3rd order Saphiro filter in order to condition steep gradients introduced by the interpolation scheme. The model's bathymetry and mask are depicted in Fig. 2. The Gibraltar Strait is located sixteen grid boxes to the east of the model's sole open boundary in the Atlantic Ocean. Right on the boundary and during each time step, the temperature and salinity is prescribed to the seasonal climatology from MED4 dataset, the latest gridded dataset provided by the Mediterranean Ocean Data Base (MODB) (Brasseur, 1995; Brasseur et al., 1996). The internal normal velocities on the boundary are governed by a Sommerfeld radiation condition and constant surface elevation is imposed as the external mode open boundary condition.

The wind stress is obtained from ECMWF data covering the period 1986–1992. The forcing is based on monthly values derived from averaging daily means of the wind stress at 10 m above the air–sea interface (Beckers et al., 1996). The climatological wind stress patterns during February and August can be observed in Fig. 3. The top layer temperature and salinity were relaxed with a restoring coefficient ($\gamma \Delta z$ Eqs. (3a) and (3b)) of 1 m day^{-1} to MED4 monthly climatology. This relaxation time scale means for example that a surface layer of 5 m needs 5 days to adjust to the climatological value. The order of magnitude of this value is similar to the ones used in other models (e.g., Tziperman and Bryan, 1993, RSAP). In the location of the Atlantic box, the applied surface forcing was linearly varied from zero for $i = 1$ to the full value right on the strait location, $i = 16$.

3. Results and discussion

The model was diagnostically span up from winter initial conditions (MED4 climatology) for three days in order to establish a horizontal flow field, and after that it was integrated for 15 years. The kinetic energy reached equilibrium after 50 months of integration. The volume average potential temperature for the whole basin is 14.5°C after 15 years of integration. The relative distribution within the subbasins is 14.0°C for the western and 14.8°C for the eastern. The increase rate of the basin was 0.05°C yr^{-1}, rate slightly higher in eastern basin. The nature of the drift is logarithmic and indicative of an increase of the heat content of the basin. Both subbasins have minimum temperature during late March and early April and maximum during October. The average basin salinity for year 15 is 38.49 psu. For West Mediterranean the salinity is 38.07 psu and for East Mediterranean, 38.74 psu. The salinity tendency of the basin is to decrease, and it is dictated by the western basin trend. This is a consequence of the combination of excessive fresh Atlantic water inflow through the Gibraltar strait and inadequate evaporation through the surface. In contrast, the eastern basin has a weak tendency for salinity increase. The different behaviour of the two subbasins has been also reported in the results of ZM. Another interesting observation is the presence of a semi-annual cycle superimposed to the annual cycle in the salinity signal, a signature of the semi-annual cycle present in the buoyancy forcing.

3.1. Surface fluxes

According to in situ observations, heat is lost on an annual basis through the surface in the Mediter-

ranean (~ 7 W m^{-2}) and the balance is kept by the inflow of relative warm Atlantic waters. In this model, there is net heat gain through the surface of about 5.8 W m^{-2}. The inflowing Atlantic waters also increase the heat content of the basin at a rate of 3.2 W m^{-2}. This contributes to the temperature increase cited above. The seasonal cycle has an amplitude value of about 70 W m^{-2} while the observed reaches 200 W m^{-2} (Garrett et al., 1993). Maximum heat loss through the surface occurs during late February and March and maximum heat gain occurs during July.

Regarding the spatial distribution of the net heat flux through the surface, the following are observed. In Fig. 4, the model's surface heat flux during February and August are shown. During winter heat is lost throughout the basin. At a higher rate is lost in northern Mediterranean, i.e., north Balearic, north Adriatic and north Aegean. Characteristic is also the heat loss in the Rhodes Gyre area. The distribution is similar to that presented by RSAP, however the loss in the Levantine is weaker. During summer, there are certain regions where heat gain is abnormally high. From the comparison of the spatial distribution of the heat flux and the wind stress pattern during the same time of the year (Fig. 3), we can conclude that the areas with high heat gain correspond to locations where strong upwelling occurs. The upwelled waters are colder than the restoring temperature from climatology and a positive surface flux is implied. Such regions are: the Aegean due to the prevailing Etesians during summer, most of the west coasts (due to northerly winds) and the North African coast (due to the westerlies). Similar but not as strong effects have been reported in RSAP. Moreover, grid size noise is present in the summer field. We believe that these are side effects of the sigma-coordinate formulation in combination with the vertical diffusivity scheme employed in this model. During winter periods of heat loss the Mellor Yamada scheme copes successfully with the surface boxes that are only a few cm deep. In the contrary, during summer when heat is gained and a shallow thermocline is present, the combination of the relaxation constant and the model's time step can be critical. Finally, another factor that is believed to be partially responsible for the incorrect heat budget is the monthly climatological forcing, as opposed to daily, and the effect it has on the mixed layer depth. Castellari and Pinardi (1994) report that when daily forcing is imposed on the RSAP model, the net heat flux through the surface initially being zero closes to -7 W m^{-2}. In ZM model, the surface flux was prescribed, and therefore, they were able to keep it to more acceptable values.

Regarding the water balance of the basin and according to the model, water is lost through the surface at a rate of 0.4 myr^{-1}. The exact value realizable in nature is not well known, but it is estimated to be in between 0.6 and 1.0 myr^{-1}. The implied excess of evaporation over precipitation is not enough to balance the salt loss through the strait of Gibraltar. The outcome is the overall freshening of the basin's water and this is reflected in the continuously decrease of the volume integrated salinity. However, as was mentioned above, this happens only in Western Mediterranean, being closest to Gibraltar, while in Eastern Mediterranean the salinity actually increases, in a very low rate though. Minimum salt flux is during May and maximum during December and March. Regarding other models, ZM imposed a surface salt flux of 1.13 myr^{-1}. Wu and Haines (1996) estimated also E–P to be around 0.4 myr^{-1}, while Pinardi et al. (1997), reported a much lower value of 0.27 myr^{-1}.

For the E–P spatial distribution we observe the following (Fig. 5): During winter, there is excessive evaporation over precipitation in water formation areas, such as the Gulf of Lions, the south Adriatic, the North Aegean and the Levantine. During summer, most of the evaporation is located in North Levantine. In North Aegean during this time of the year precipitation exceeds evaporation, indication of the increased Black Sea outflow. Also we observe freshwater gain along the Algerian coasts throughout the year. It seems that at locations with cyclonic variability there is salt gain whereas the opposite is true in areas with anticyclonic activity. The spatial distribution in nature is not well known. From bulk formulae and COADS dataset we have estimated the evaporation component. According to this (not shown), the evaporation is strong in South Aegean and Northern Balearic Sea (Lions Gulf), in agreement with the model results. However, if the precipitation from climatology is taken into account, its characteristic latitudinal distribution prevails and

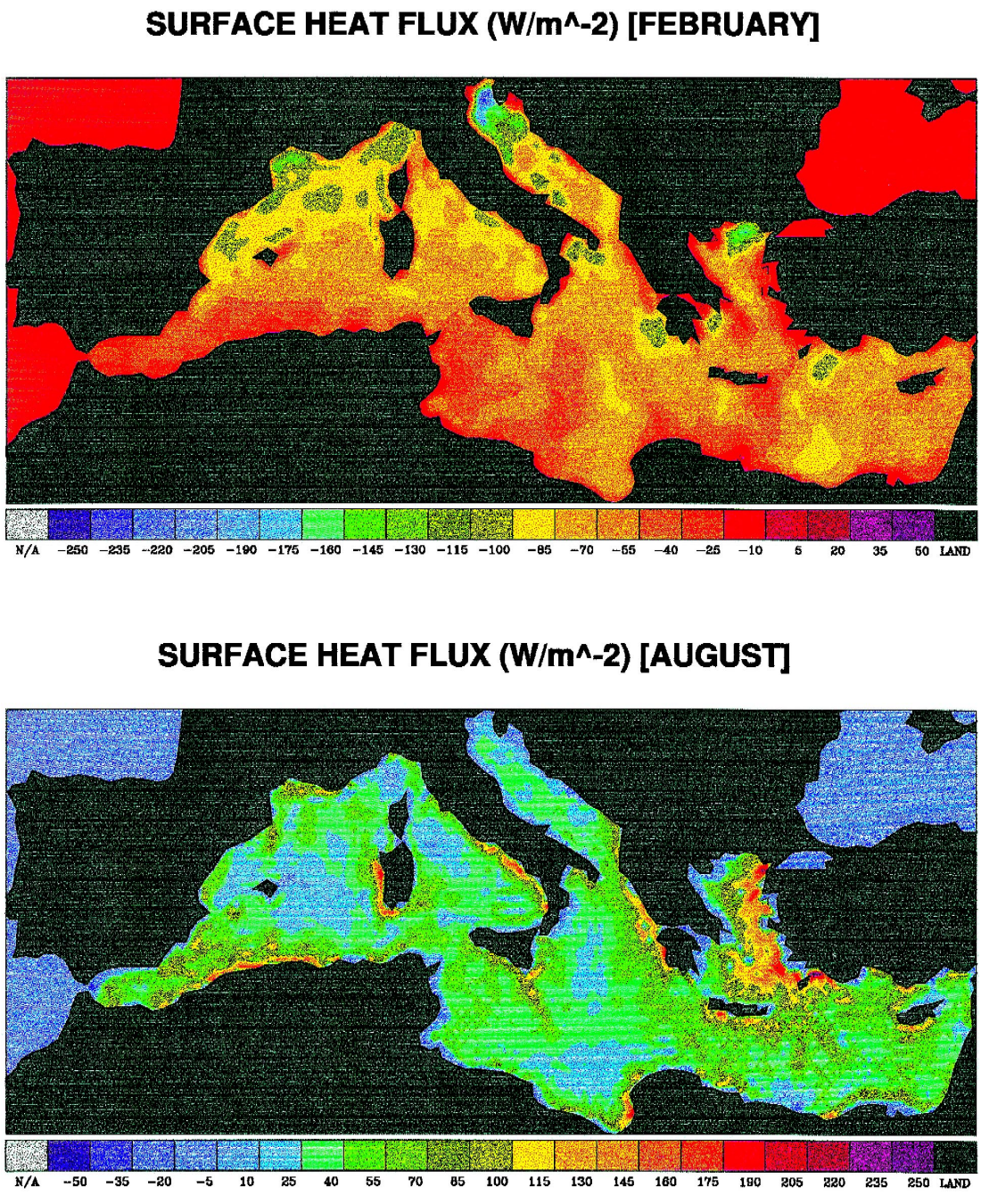

Fig. 4. Implied surface heat fluxes in W/m^2. (a) February, (b) August.

masks the distribution mentioned above. It should be also noted, that the standard deviation of the E–P variability is much stronger in the model.

A final note on the fluxes: When the seasonal signal is filtered from the time series of net heat flux and E–P, there is a trend of reduction in the former

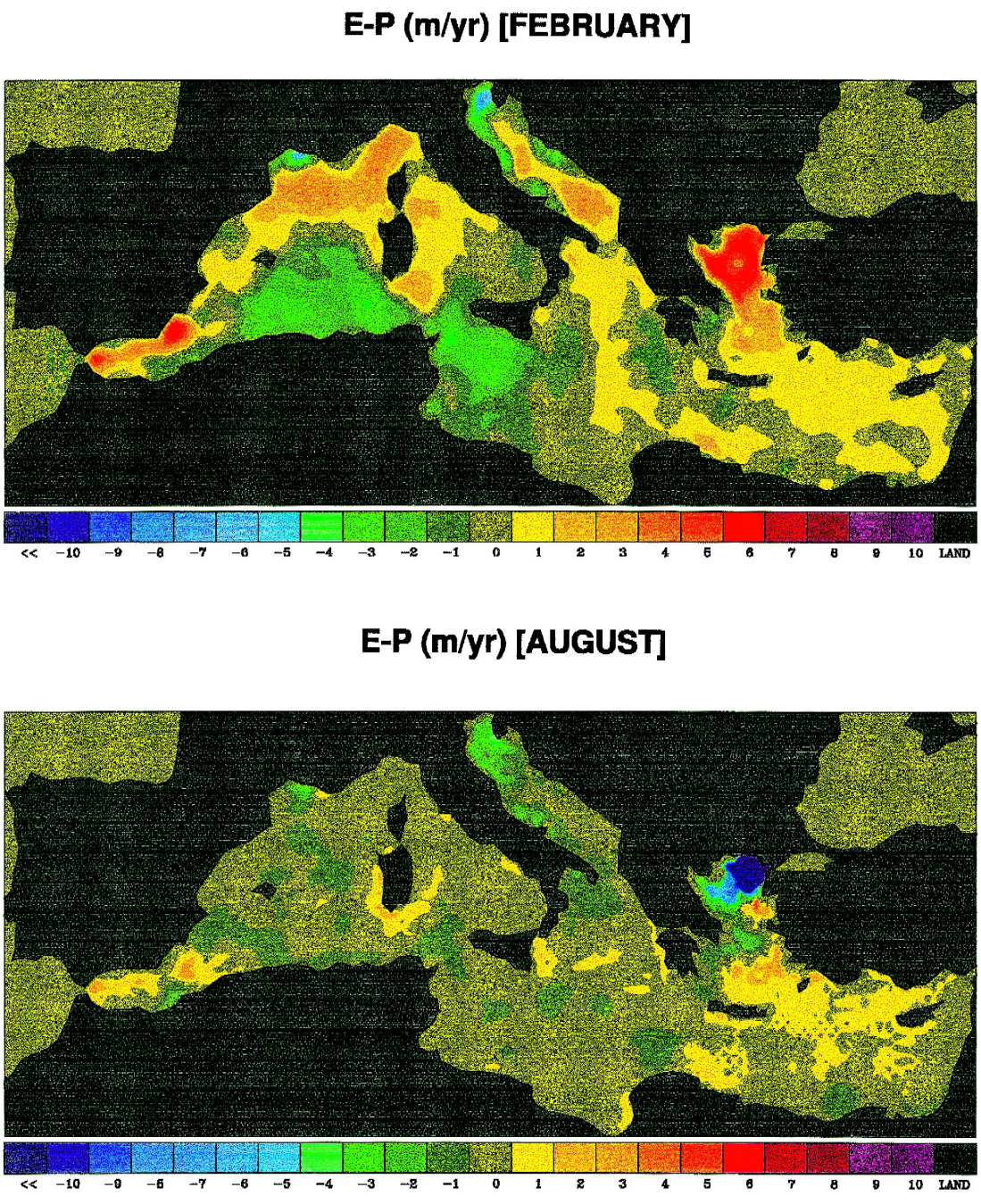

Fig. 5. Implied surface water fluxes in myr^{-1}. (a) February (b) August.

and increase in the latter. These trends are in the right direction, hinting that on the long run the model might reach a more realistic steady state, in terms of heat and salt fluxes.

3.2. General circulation

In order to describe the basin's general circulation based on the results of the present model, three parameters are examined. The free surface elevation which is indicative of the upper thermocline circulation, the barotropic stream function for assessing the barotropic transport component, and the eulerian velocity field for describing the flow patters and variability as a function of depth. For the last parameter three depths are chosen: For the surface circulation the depth of 5 m, for the intermediate water circulation 280 m, and for deeper circulation 620 m. The seasonality of the flow field is resolved by describing the fields during February (winter conditions) and August (summer conditions).

The free surface elevation for winter conditions is shown in Fig. 6a. All major circulation features described in the Introduction are present. The Algerian current stays close to the north African coast meandering and generating a series of anticyclonic features. The circulation in most of the Balearic Sea is cyclonic and the Lyons Gyre is well defined. The flow in the Tyrrhenian is also cyclonic, consisting of a branch of the Atlantic water which appears to pile up against the west coast of Italy. In the Gulf of Syrte two anticyclones are present, part of the meandering Ionian Current. The flow in the Ionian is cyclonic with the North Ionian cyclonic gyre well defined. A series of cyclones are also present in the Adriatic Sea. The Ionian current which evolves in the Mid Mediterranean Jet in the Levantine, seems to travel around the island of Cyprus. The circulation in the North Levantine is cyclonic and seems that there exist two cyclonic gyres in the area south of the Island of Rhodes, presumably a combination of the Rhodes and West Cyprus Gyres (Robinson and Golnaraghi, 1993). The Mersa–Matruh anticyclone, located near the coast of Egypt is also formed. During summer (Fig. 6b), there are some changes in the upper layer flow. The Algerian Current extends northward and the circulation in the Tyrrhenian changes to clearly anticyclonic. This has also been reported by RSAP and by Tziperman and Makanotte-Rizzoli (1991). Similarly in the Ionian, the Ionian current extends in northern Ionian and its meandering creates an anticyclonic flow, a feature which has been reported by the inverse model of Tziperman and Makanotte-Rizzoli (1991), but this is the first time it has been successfully reproduced in a numerical model. The Rhodes Gyre is still present but it is not extending as much westward. The Mersa–Matruh Gyre is well defined. In the Aegean, due to the Etesians blowing from north (see Fig. 3b), the free surface elevation is low along the Asia Minor coasts.

The barotropic transport is presented in Fig. 7. The flow patterns show low seasonal variability. Most predominant features are anticyclonic. Such features are a series of anticyclones along the Moroccan and Algerian coasts and a permanent anticyclonic barotropic gyre in the Tyrrhenian. This gyre is much weaker during winter, and due to the baroclinic flow of the Modified Atlantic Water (MAW) at that time of the year in the area the flow reverses sense of rotation. In the eastern Mediterranean and in the Ionian the flow has a cyclonic component in the center surrounded by a series of anticyclones. A well known anticyclone the Pelops Gyre off the west coast of Peloponnesus emerges clearly. The Mersa–Matruh Gyre is also present but it is better defined in summer. Another well known anticyclone that has been successfully reproduced in a model for the first time to the best of our knowledge is the Antalya Gyre in the Gulf of Antalya in south Asia Minor, north of Cyprus.

The total flow field for the three distinctive depths is presented in Fig. 8 for winter and in Fig. 9 for summer. During winter near the surface the flow pattern is characteristic of the Atlantic water system. In the western subbasin a meandering strong current propagates along the Algerian coast. When it reaches the east coast of Sardinia it bifurcates, and a section heads up in the Tyrrhenian where through the Strait of Corsica enters in the Ligurian and North Balearic and creates a strong Ligurian–Provencal Current. This current eventually reaches the Alboran Sea. This circulation of waters of Atlantic origin is in a good agreement with the picture presented by Millot (1987), which is based on in situ measurements. The major section of MAW enters the eastern Mediterranean generating the Ionian Current and eventually rejoins the North African coast near the Cretan passage. There it evolves into the Mid Mediterranean Jet which bifurcates near Egypt with one section heading northward near the island of Cyprus and the other reaching the coast of Israel and then heading

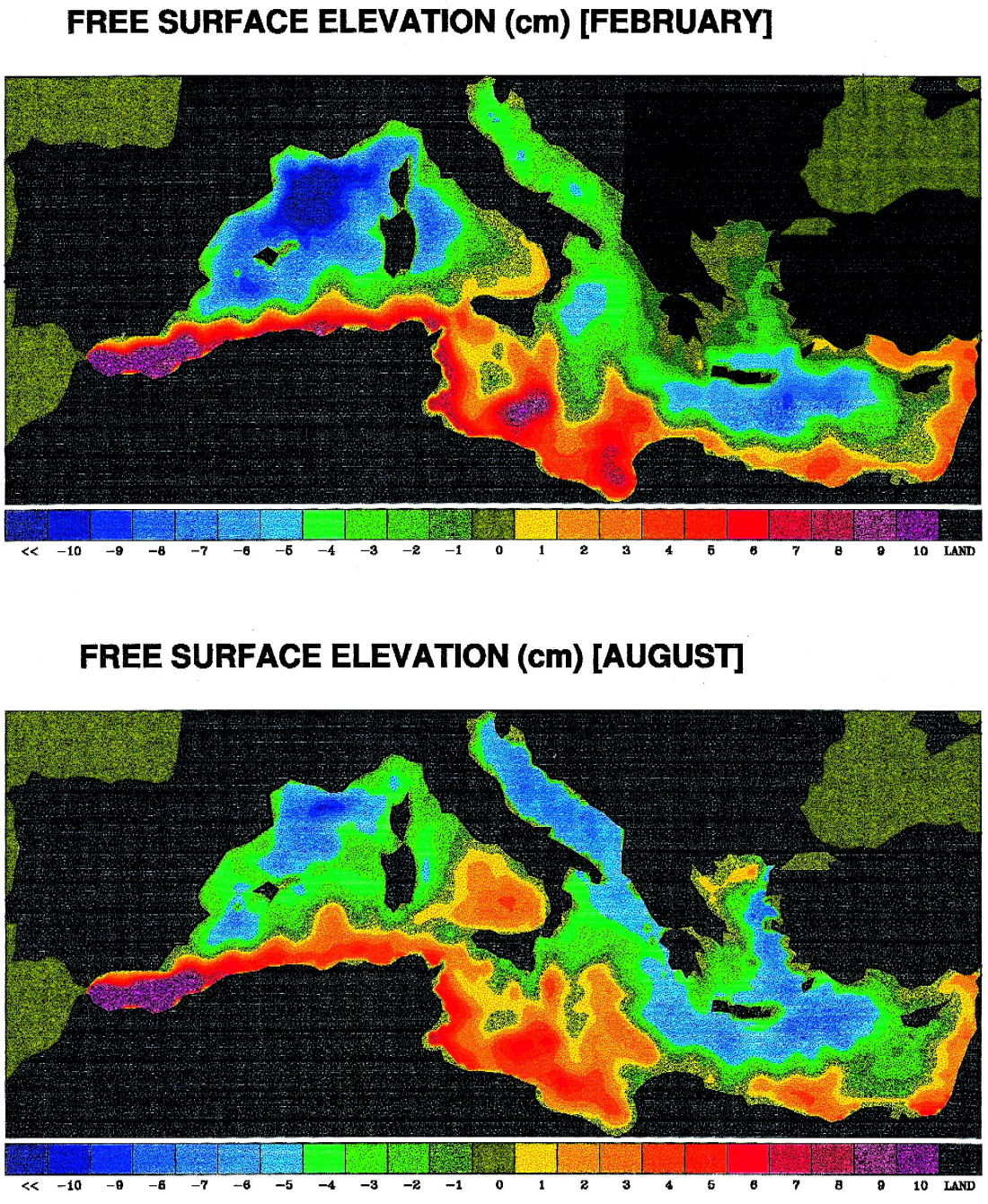

Fig. 6. Free surface elevation in cm. (a) February, (b) August.

northward to rejoin the former and to create the Asia Minor current. The current enters the Cretan Sea through the Straits of Karpathos and most outflows through the eastern Strait of Kithira. On either side of the main body of the Mid Mediterranean Jet the Rhodes and Mersa–Matruh Gyres are present. In

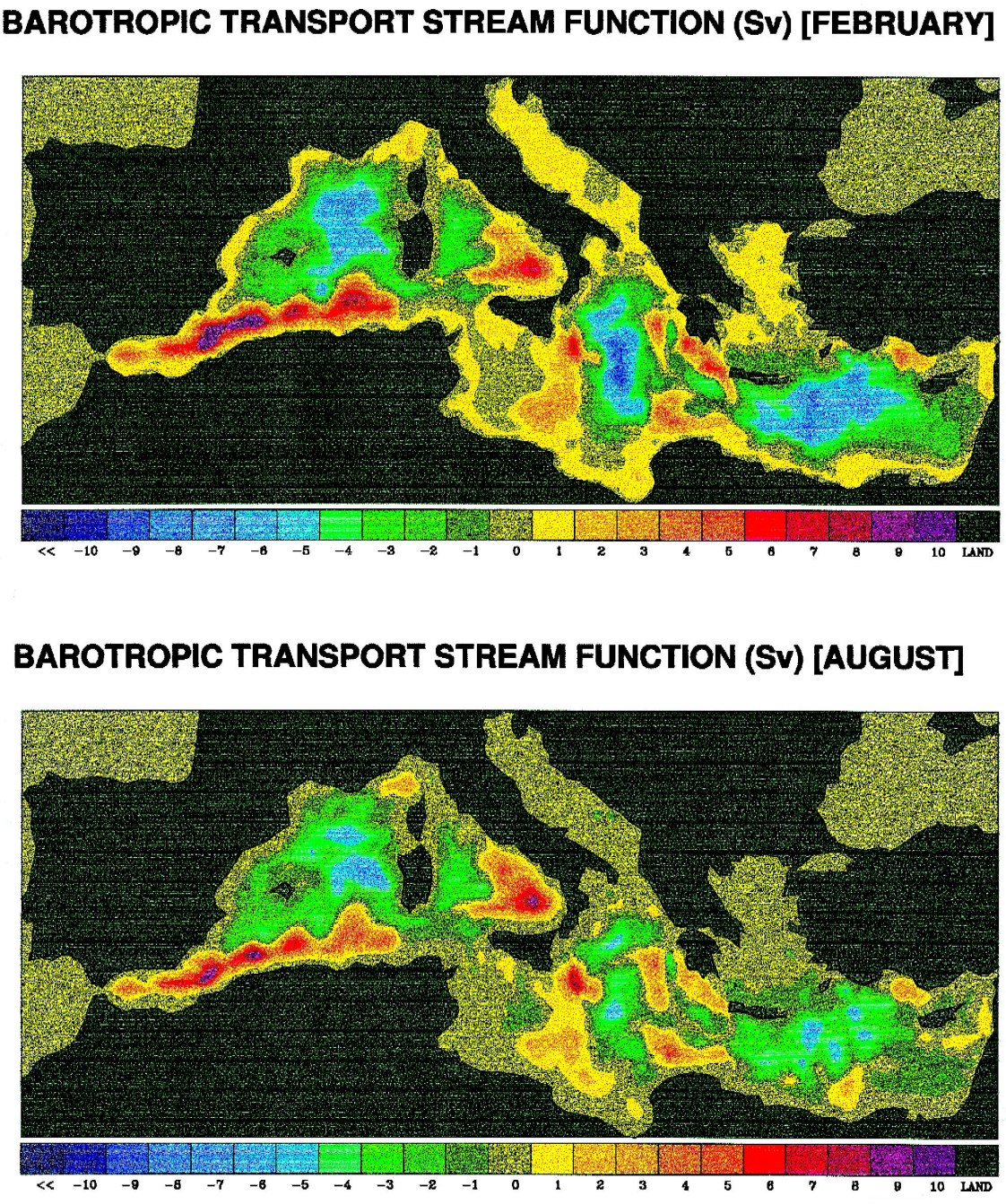

Fig. 7. Barotropic stream function in Sv. (a) February, (b) August.

southern Adriatic a cyclonic gyre is formed in good agreement with the inverse model of Tziperman and Makanotte-Rizzoli (1991). At the depth of 280 m where intermediate water flows, the exported East Mediterranean waters enter Tyrrhenian and following a cyclonic path reach Corsica. One section propagates through Corsica Strait, the other flows around Corsica and Sardinia and rejoins the former at the

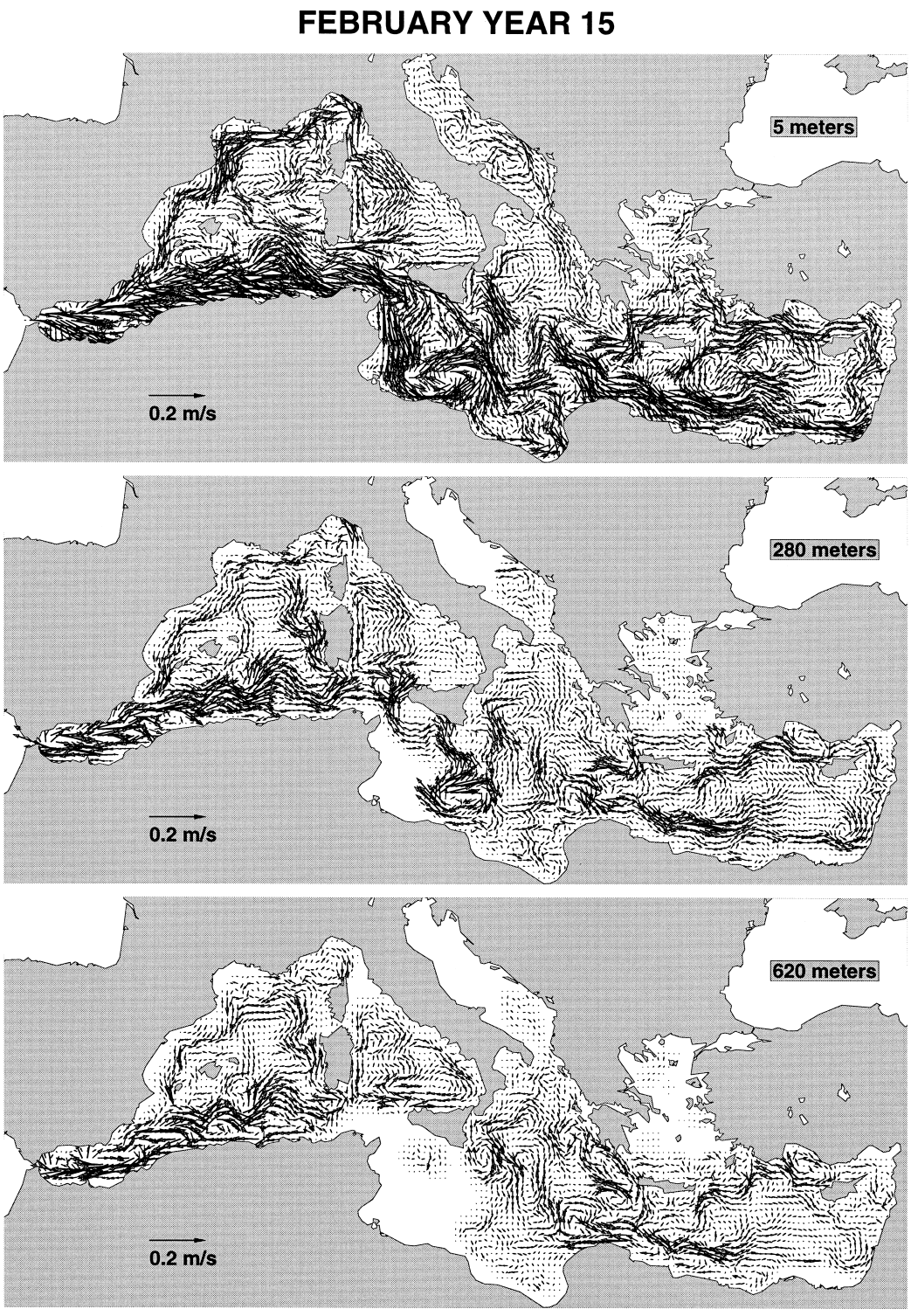

Fig. 8. Velocity vectors during February for three depths: 5 m, 280 m, 620 m. The units are cm/s.

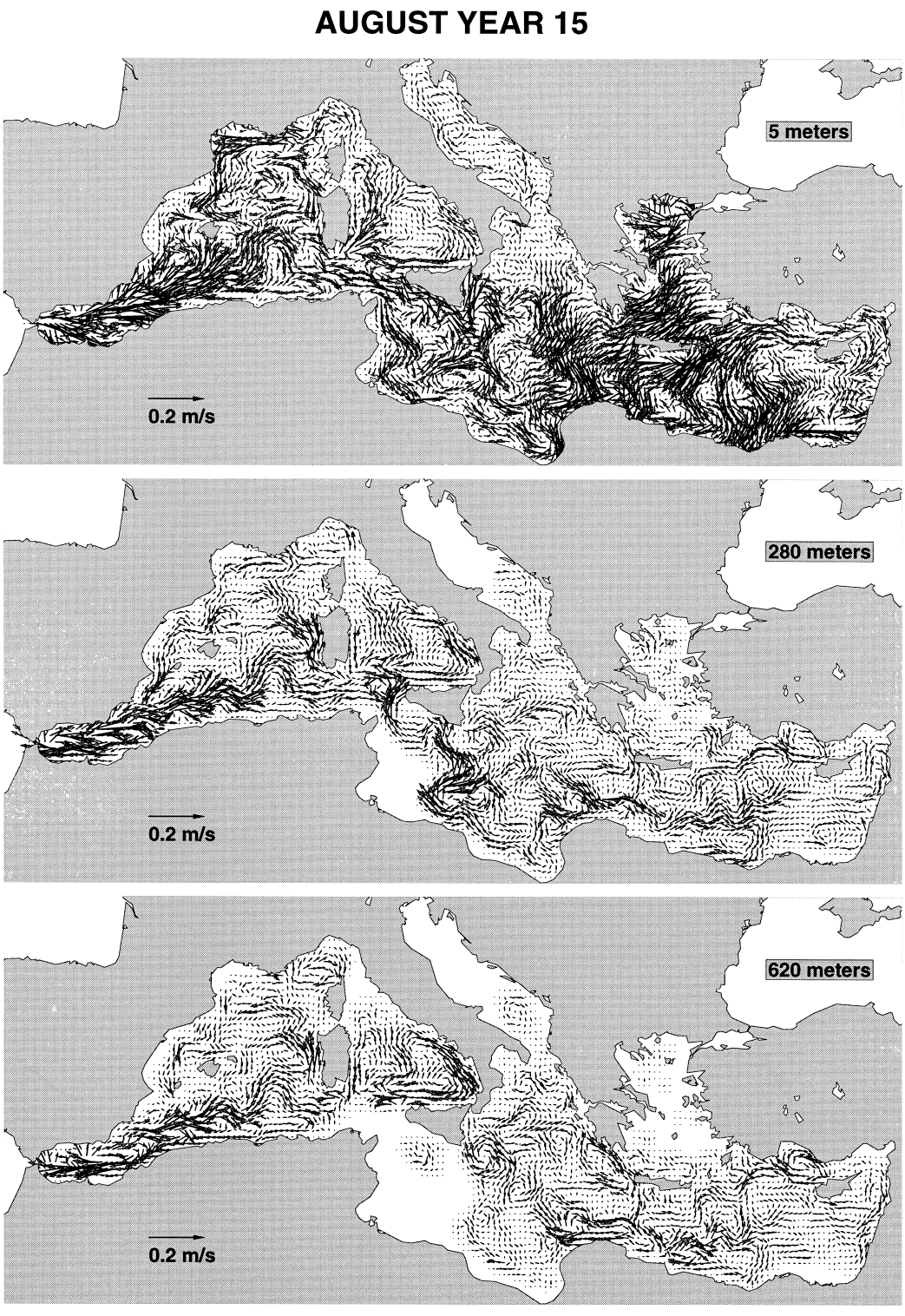

Fig. 9. Velocity vectors during August for three depths: 5 m, 280 m, 620 m. The units are cm/s.

Lyons Gyre location. This picture again is in a good agreement with that presented by Millot (1987). At the depth of 620, the Algerian Current is still strong, and flow in Tyrrhenian has turned to anticyclonic due to the strong barotropic component. Some of the deep features are more clear. The flow of eastern Mediterranean waters along the east coast of Corsica and Sardinia which then head towards the Gulf of Lions and north of Majorca to exit eventually through Gibraltar Strait. In eastern Mediterranean the Antalya Gyre is the predominant feature.

During summer, the flow at the surface is weaker in western Mediterranean. The Algerian Current in certain regions moves away from the Algerian coast in the southern Balearic basin and at one point bifurcates with one section heading northward. The other section, after passing Sardinia bifurcates again with one section entering the Tyrrhenian while the main stream enters East Mediterranean through Sicily Strait. In the Gulf of Lions, there is a well defined Ligurian–Provencal current. The flow now in the Tyrrenian Sea is clearly anticyclonic. The Ionian current is strongly meandering, creating cyclones and anticlones. A very strong anticyclone is present in the Gulf of Syrte. In Levantine, the flow is cyclonic and the Asia Minor Current present, although the flow now is around the west coast of Cyprus. Compared to winter conditions, the flow in the Aegean is intensified due to the Etesians, and is southward, with strong outflow through Kithira strait. At 280 m, there is outflow from Eastern Med through Sicily strait to Western basin, some of which is heading in the Tyrrhenian and Corsica strait and possibly returning south to reunite with the main flow. The main body flows northward in Balearic basin, along the west coast of Sardinia. Flow in western Peloponnesus is southward, and the Pelops Gyre clearly emerges. The Antalya anticyclone is a predominant feature in the Levantine, and the Mersa–Matruh and Rhodes Gyres are present, separated by the meandering Mid Mediterranean Jet. At the depth of 620 m there are no major changes compared to winter, an indication of no deep water formation.

3.3. Thermohaline circulation and straits

The most characteristic water masses in the Mediterranean are the deep waters of the eastern and western basins, and the intermediate waters in the Levantine. All these masses are formed during winter, through different processes, which are difficult to be reproduced in a coarse resolution climatologically forced model. The lack of formation of water masses with correct properties and the resulting unrealistic thermohaline circulation in this model, comes as no surprise therefore.

One of the most important water masses in the Mediterranean is the Levantine Intermediate Water (LIW). This mass is believed to be formed in the doming area of Rhodes Gyre during winter and settles at depths of about 300–500 m (Lascaratos et al., 1993). Its importance lies with the fact that during its spreading phase reaches the basin's deep water formation areas and being extreme saline (39 psu) helps in the preconditioning of the water column. Moreover, the water mass that actually outflows from Gibraltar is mainly composed of LIW. In this model, during March and early April, intermediate water is formed at Rhodes Gyre and the surrounding area. Its potential density is around 28.55, lower than the observed 29. This is a result of not enough buoyancy loss in the formation area. Formation occurs down to 320 m at the doming area of the cyclone. The salinity is 38.85 psu and the temperature 16.6°C. From observations, this mass should have temperature around 15.5°C. However no model up today has been able to produce LIW with such characteristics under realistic forcing conditions.

It is believed that in East Mediterranean, deep waters (EMDW) are formed on the shallow shelf of north Adriatic and eventually slide down to South Adriatic and through Otranto to the deepest areas of Ionian and Levantine. Moreover, Ovchinikov et al. (1987), observed that during that particular winter, EMDW is formed in the center of the cylonic gyre in south Adriatic and eventually slide to settle in the deepest areas of the Ionian and Levantine basins. Although this gyre is present in our model, the preconditioning of the water column in South Adriatic by the LIW is not enough to drive open ocean convection. A transient water mass with density of 28.8 is formed in North Adriatic which slides to South Adriatic and to the Ionian to settle to depths ranging from 250 to 500 m.

In the Western Mediterranean and in the area of Lyons Gyre, another characteristic water mass is

formed, the West Mediterranean Deep Water (WMDW). It has density 29.1, temperature 12.7°C and salinity 38.4 psu. This water mass is formed through open ocean deep convection during extreme cooling episodes in winter, and spreads in the deepest parts of the western basin. Such process is difficult to be reproduced in models forced with climatological surface boundary conditions (as opposed to daily). In this location, only the modeling effort of Wu and Haines (1996) was successful in producing such water masses. It was achieved by incorporating a combination of a rather strong relaxation scheme and low restoring temperatures, which resulted in extreme heat loss locally. This model, during March and April, forms a transient water mass at the dome of Lyons Gyre, and at a depth of about 600 m with potential density of 28.6. The salinity is 38.02 psu and the temperature is 14.4°C. It should be also stressed here that although LIW reaches in the formation site, due to its low salinity the preconditioning of the water column is inadequate.

The straits play an important role in controlling both the general and the thermohaline circulation in the Mediterranean (Table 1). The overall flow of the basin is controlled via the Strait of Gibraltar, which acts as a valve for the inflow of Atlantic and outflow of Mediterranean waters. Based on the model, the volume transport of each layer is about 1.2 Sv. From field measurements this value should be around 0.7 to 1.3 Sv depending on the reference (Bryden et al., 1996; Lacombe and Richez, 1982). Although the net transport is mainly controlled by the buoyancy loss in the basin, the local width of the strait should have an effect on the transport. Due to modeling limitations, the strait was represented by two $1/4° \times 1/4°$ boxes, and this is expected to reduce the role of friction. It is interesting to note that in ZM despite the better resolved strait (8 km), even higher transports (1.3 Sv) were obtained. In RSAP the exchange is 0.8 Sv. The net outflow of salt is 1.45 psu Sv, very close to the value of 1.5 psu Sv cited in Bryden et al. (1996). The heat input from the strait, due to the inflowing warmer Atlantic water is about 3.2 W m^{-2} (normalized over the whole surface of the basin).

Table 1
Annual volume, heat, and salt transports in important straits. The directions of flow are in parentheses

Strait	Volume transport (Sv)	Heat transport ($\times 10^{12}$ J s^{-1})	Salt transport (psu Sv)
Gibraltar	1.19 (–)	7.5 (E)	1.45 (W)
Corsica	0.77 (N)	47.5 (N)	29.13 (N)
Sicily	1.96 (–)	3.2 (E)	0.51 (W)
Otranto	0.44 (–)	1.3 (N)	0.01 (S)
Kithira	1.23 (S)	81.7 (S)	47.36 (S)
Karpathos	1.23 (S)	81.0 (N)	47.91 (N)

The Sicily Strait controls the exchange between the two subbasins. The model indicates a volume transport of almost 2 Sv (standard deviation 0.1 Sv). Maximum exchange is from November till February as is observed by most in situ measurements (e.g., Grancini and Michelato, 1987; Manzella et al., 1988; Astraldi et al., 1996). In these references, the quoted transport value ranges from 1.2 to 3 Sv. Wu and Haines (1996) estimated the exchange in their model to be 0.7 Sv. The net westward salt transport is 0.5 psu Sv, less than half the value of 1.3 psu Sv reported in Moretti et al. (1993) and similar to the value 0.7 psu Sv reported in Pinardi et al. (1997). The low salinity transport can be attributed to the lack of intermediate water formation of the right salinity (39 psu) in the Levantine basin area. The heat transport is westward as expected and about 3.2×10^{12} J s^{-1} much higher than the value of 0.6×10^{12} J s^{-1} reported in Moretti et al. (1993) than the value of 10.7×10^{12} J s^{-1} reported in Pinardi et al. (1997).

For the Otranto Strait, the model implies an annual exchange of 0.4 Sv (standard deviation 0.1 Sv), while it has been reported an observed value of about 0.3 Sv by Zore-Armanda and Pucher-Petkovic (1976) and 0.4 Sv by Wu and Haines (1996). Maximum exchange is during October. The net heat transported to the west is 1.3×10^{12} J s^{-1}, due to the inflow of relatively warm waters from Ionian, while salt transport is 0.01 psu Sv, due to the saltier deep waters leaving the Adriatic.

Almost all the transport through Corsica strait is northward, with an annual mean of 0.8 Sv. It has a very strong seasonal cycle (0.3 Sv standard deviation). The northward transported waters transfer heat flow of some 70×10^{12} J s^{-1}. Salt is also flowing northward (29 psu Sv).

Two more straits have been the center of attention lately. These are the Kithira Strait located between

western Crete and the southmost tip of Peloponnesus and the Karpathos Strait located in between the eastern Crete and the island of Rhodes. These straits join the Aegean Sea with the Ionian and Levantine basins and therefore control the water mass exchange between the subbasins. The reason of the attention has to do with the fact that recently, major changes have been observed in the properties of the Aegean waters outflowing to the Ionian and Levantine basins (Roether et al., 1996). According to these observations, the Aegean waters have become heavy enough to replace the bottom waters in Eastern Mediterranean originating from the Adriatic Sea.

According to this model, there is a net inflow to the Aegean of 1.2 Sv through the eastern strait, and an outflow of 1.2 Sv through the western strait. The transported heat from east due to the inflow is about 8.1×10^{13} J s^{-1}. As a consequence, about 8.2×10^{13} J s^{-1} are exported in the Ionian and Levantine basins through Kithira strait in the West. This balance corresponds to a net heat gain in the Aegean through the surface. As it has been mentioned above, this is the outcome of the strong upwelling in the Aegean combined with the relaxation scheme. Finally, there is a net salt gain in the Aegean from the Eastern Strait (47.9 psu Sv) and net salt loss from the Western Strait (47.4 psu Sv).

4. Conclusions

In this paper, we have presented a new modelling effort for the circulation of the Mediterranean Sea. The focus of this work was twofold; to try to emulate as realistically as possible the general circulation as we know it up to this day, and to understand the driving mechanisms behind these circulation features. This model as such has been able to reproduce most of the known features present in the mean circulation of the upper thermocline. In addition, some of them have been reproduced for the first time in a GCM. These include the change of flow from cyclonic to anticyclonic in North Ionian, the Antalya Gyre, the Pelops Gyre and a well defined Ligurian–Provencal Current. It was shown that most of the known patterns have a strong barotropic component (i.e., are wind driven). The seasonality of the model's circulation was in accordance with the observations. Moreover an overall realistic transport through the straits was achieved. The seasonal signal of the transports in Gibraltar was negligible.

This model was not able to form deep waters. We believe that the main reason behind this is the low temporal resolution of the forcing fields. Evidence from other modelling efforts points to the importance of daily forcing in GCMs in order to reproduce a mixed layer of proper depth. Another reason could have been the value of the restoration coefficient. In order to assess the importance of its magnitude we have performed another experiment with double the relaxation constant (2 m day^{-1}). The annual mean surface heat flux was found to improve no more than 30%. The salt flux was almost identical and a minor improvement was observed in the hydrographic properties. The absence of mesoscale physics in this model (the Rossby radius of deformation for the Mediterranean is 10 km) and the resulting interaction of the eddy field with the mean flow has certainly an effect on the dispersal of the newly formed water masses (Wu and Haines, 1996) and on the preconditioning of water column in the deep water formation areas.

In Part II of this modelling effort, an eddy resolving $1/8° \times 1/8°$ in longitude and latitude will be presented forced with daily atmospheric forcing and interactive fluxes.

Acknowledgements

This work has been supported through EU concerted action MAS2-CT94-0107. Useful comments by two anonymous referees are acknowledged.

References

Astraldi, M., Gasparini, G.P., Sparnocchia, S., Moretti, M., Sansone, E., 1996. The characteristics of the water masses and the water transport in the Sicily Channel at long time scales. Bulletin de l'Institut Oceanographique Monaco 17, 37–57.

Beckers, J.-M., Schmitz, F., Brasseur, P., Brankart, J.M., Crepon, M., Herbaut, Ch., Martel, F., Van den Berghe, F., Lascaratos, A., Drakopoulos, P.G., Pinardi, N., Carini, P., Tintore, J., Alvarez, A., Parrilla, D., Vautard, R., Speich, S., 1996. First annual report of the Mediterranean models evaluation experiment, MEDMEX. Project reports, Commission of European Union, Brussels.

Bethoux, J.P., 1979. Budgets of the Mediterranean Sea. Their dependence on the local climate and on the characteristics of the Atlantic waters. Oceanol. Acta 2, 157–163.

Blumberg, A.F., Mellor, G.L., 1987. A description of a three-dimensional coastal ocean circulation model, three-dimensional coastal ocean models. In: Heaps, N.S. (Ed.), Coastal Estuarine Science, Agu, 1–16.

Bryden, H.L., Kinder, T.H., 1991. Steady two-layer exchange through the strait of Gibraltar. Deep-Sea Res. Part A 38S, 5445–5463.

Bryden, H.L., Candela, J., Kinder, T.H., 1996. Exchange through the Strait of Gibraltar. Prog. Oceanogr. 33, 201–248.

Brasseur, P., 1995. Free data offered to researchers studying the Mediterranean. Eos 76, 363.

Brasseur, P., Beckers, J.M., Brankart, J.M., Schoenauen, R., 1996. Seasonal temperature and salinity field in the Mediterranean Sea: climatological analyses of a historical data set. Deep-Sea Res. 43, 159–192.

Castellari, S., Pinardi, N., 1994. A new perpetual year model of the Mediterranean circulation, Tech. Rep., 1–94, Ist. Per lo Stud. Delle Meted. Geofis. Ambient., Modena, Italy.

Crepon M., Martel, F., 1996. Euromodel II: The Hydrodynamics of the Western Mediterranean. In: Weydert, M., Lipiatou E., Goni, R., Fragakis, C., Bohle-Carbonell, M., Barthel, K.-G. (Eds.), Second Mast Days and Euromar Market, Vol. 1 of Project reports, Commission of the European Communities, Brussels, pp. 480–493.

Garrett, C., Outerbridge, R., Thomson, K., 1993. Interannual variability in Mediterranean heat and buoyancy fluxes. J. Clim. 6, 900–910.

Grancini, G.F., Michelato, A., 1987. Current structure and variability in the Strait of Sicily and adjacent area. Ann. Geophys. 5B, 75–88.

Lacombe, H., Richez, C., 1982. The regime of the Strait of Gibraltar. In: Nihoul, J.C.J. (Ed.), Hydrodynamics of Semi-Enclosed Seas. Elsevier, Amsterdam, pp. 13–73.

Lascaratos, A., Williams, R.G., Tragou, E., 1993. A mixed-layer study of the formation of Levantine Intermediate Water. J. Geophys. Res. 98, 14739–14749.

Malanotte-Rizzoli, P., Bergamasco, A., 1989. The general circulation of the eastern Mediterranean: I. The barotropic wind driven circulation. Oceanol. Acta 12, 335–351.

Malanotte-Rizzoli, P., Bergamasco, A., 1991. The wind and thermally driven circulation of the eastern Mediterranean Sea: II. The baroclinic case. Dyn. Atmos. Oceans 15, 355–419.

Manzella, G.M.R., Gasparini, G.P., Astraldi, M., 1988. Water exchange between the eastern and western Mediterranean through the Strait of Sicily. Deep-Sea Res. 35, 1021–1035.

Mellor, G.L., Yamada, T., 1982. Development of a turbulent closure model for geophysical fluid problems. Rev. Geophys. 20, 851–875.

Menzin, A.B., Moskalenko, L.V., 1982. Calculation of wind-driven currents in the Mediterranean Sea by the electrical simulation method (homogeneous model). Oceanolography 22, 537–540.

Millot, C., 1987. Circulation in the Western Mediterranean Sea. Oceanol. Acta 10, 143–149.

Moretti, M., Sansone, E., Spezie, G., De Maio, A., 1993. Results of investigations in the Sicily Channel (1986–1990). Deep-Sea Res. 40, 1181–1192.

Ovchinikov, I.M., Zats, V.I., Krivosheya, V.G., Nemirovsky, M.S., Udodov, A.I., 1987. Winter convection in the Adriatic and formation of deep eastern Mediterranean waters. Ann. Geophys., Ser. B 5B, 89–92.

Pinardi, N., Navarra, A., 1993. Baroclinic wind adjustment processes in the Mediterranean Sea. Deep Sea Res. 40, 1299–1326.

Pinardi, N., Korres, G., Lascaratos, A., Roussenof, V., Stanev, E., 1997. Interannual variability of the Mediterranean Sea. Geophys. Res. Lett., in press.

Robinson, A.R., Golnaraghi, M., 1993. Circulation and dynamics of the Eastern Mediterranean Sea; quasi-synoptic data-driven simulations. Deep-Sea Res. II, 40, pp. 1207–1246.

Robinson, A.R., Golnaraghi, M., 1994. The physical and dynamical oceanography of the Mediterranean Sea. In: Malanotte-Rizzoli, P., Robinson, A.R. (Eds.), Ocean Processes in Climate Dynamics: Global and Mediterranean Examples. Kluewer Academy, Norwell, MA. pp. 255–306.

Roether, W., Manca, B.B., Klein, B., Bregant, D., Georgopoulos, D., Beitzel, V., Kovacevic, V., Luchetta, A., 1996. Recent changes in Eastern Mediterranean deep waters. Science 271, 333–335.

Roussenov, V., Stanev, E., Artale, V., Pinardi, N., 1995. A seasonal model of the Mediterranean Sea general circulation. J. Geophys. Res. 100, 13515–13538.

Smagorinsky, J., 1963. General circulation experiments with the primitive equations: I. The basic experiment. Monthly Weather Review 91, 99–164.

Stanev, E.V., Friedrich, H.J., Botev, S., 1989. On the seasonal response of intermediate and deep water to surface forcing in the Mediterranean Sea. J. Phys. Oceanogr. 12, 141–149.

Tziperman, E., Makanotte-Rizzoli, P., 1991. The climatological seasonal circulation of the Mediterranean Sea. J. Mar. Res. 49, 411–434.

Tziperman, E., Bryan, K., 1993. Estimating global air–sea fluxes from surface properties and from climatological flux data using an oceanic general circulation model. J. Geophys. Res. 98, 22629–22644.

Wu, P., Haines, K., 1996. Modeling the dispersal of Levantine Intermediate Water and its role in Mediterranean deep water formation. J. Geophys. Res. 101, 6591–6607.

Zavatarelli, M., Mellor, G.M., 1995. A numerical study of the Mediterranean Sea circulation. J. Geophys. Res. 25, 1384–1414.

Zore-Armada, Pucher-Petkovic, 1976.